Corrections to finite–size scaling in the φ^4 model on square lattices

J. Kaupužs[1,2] * , R. V. N. Melnik[3], J. Rimšāns[1,2,3]

[1]Institute of Mathematics and Computer Science, University of Latvia
29 Raiņa Boulevard, LV–1459 Riga, Latvia
[2] Institute of Mathematical Sciences and Information Technologies,
University of Liepaja, 14 Liela Street, Liepaja LV–3401, Latvia
[3] The MS2 Discovery Interdisciplinary Research Institute,
Wilfrid Laurier University, Waterloo, Ontario, Canada, N2L 3C5

May 15, 2015

Abstract

Corrections to scaling in the two–dimensional scalar φ^4 model are studied based on non–perturbative analytical arguments and Monte Carlo (MC) simulation data for different lattice sizes L ($4 \leq L \leq 1536$) and different values of the φ^4 coupling constant λ, i. e., $\lambda = 0.1, 1, 10$. According to our analysis, amplitudes of the nontrivial correction terms with the correction–to–scaling exponents $\omega_\ell < 1$ become small when approaching the Ising limit ($\lambda \to \infty$), but such corrections generally exist in the 2D φ^4 model. Analytical arguments show the existence of corrections with the exponent 3/4. The numerical analysis suggests that there exist also corrections with the exponent 1/2 and, very likely, also corrections with the exponent about 1/4, which are detectable at $\lambda = 0.1$. The numerical tests clearly show that the structure of corrections to scaling in the 2D φ^4 model differs from the usually expected one in the 2D Ising model.

Keywords: φ^4 model, corrections to scaling, Monte Carlo simulation

1 Introduction

The φ^4 model is one of the most extensively used tools in analytical studies of critical phenomena – see, e. g.,[1–7]. These studies have risen also a significant interest in numerical testing of the theoretical results for this model. Recently, some challenging non–perturbative analytical results for the corrections to scaling in the φ^4 model have been obtained [8], which could be relatively easily verified numerically in the two–dimensional case. Therefore, we will further focus just on this case. Although the analytical studies are based on the continuous φ^4 model, its lattice version is more convenient for Monte Carlo (MC) simulations. Earlier MC studies of the 2D lattice model go back to the work by Milchev, Heermann and Binder [9]. The continuous version has been simulated, e. g., in [10]. In [9], effective critical exponents $\nu \approx 0.8$ for correlation length and $\gamma \approx 1.25$ for susceptibility have been obtained, based on the simulation data for lattices sizes up

---

to $L = 20$. The considered there a scalar 2D φ^4 model should belong to the 2D Ising universality class with the exponents $\nu = 1$ and $\gamma = 7/4$, so that these effective exponents point to the presence of remarkable corrections to scaling. A later MC study [11] of larger lattices, up to $L = 128$, has supported the idea that this model belongs to the 2D Ising universality class, stating that the asymptotic scaling is achieved for $L \gtrsim 32$. Apparently, numerical studies cause no doubts that the leading scaling exponents for the two–dimensional scalar φ^4 model and the 2D Ising model are the same. However, it is still important to refine further corrections to scaling. Indeed, the 2D φ^4 model can contain nontrivial correction terms, which do not show up or cancel in the 2D Ising model. We will focus on this issue in the following sections.

2 Analytical arguments

In [8], a theorem has been proven concerning corrections to scaling in the continuous φ^4 model, based on a set of assumptions, i. e., certain conditions stated in the theorem. Based on this theorem, it has been argued in [8] that the two–point correlation function contains a correction term with the correction–to–scaling exponent $\theta_\ell = \gamma - 1$ if $\gamma > 1$ holds for the susceptibility exponent γ. Here we reconsider these non–perturbative analytical arguments by proving a new theorem, leading to the same conclusions at even better (softer) natural assumptions, which have been verified numerically.

We consider the continuous φ^4 model in the thermodynamic limit of diverging volume $V \to \infty$ with the Hamiltonian $\mathcal{H}$ given by

$$\frac{\mathcal{H}}{k_B T} = \int \left(r_0 \varphi^2(\mathbf{x}) + c(\nabla \varphi(\mathbf{x}))^2 + u \varphi^4(\mathbf{x}) \right) d\mathbf{x} \,, \tag{1}$$

where the order parameter $\varphi(\mathbf{x})$ is an n–component vector with components $\varphi_i(\mathbf{x})$, depending on the coordinate $\mathbf{x}$, T is the temperature, and k_B is the Boltzmann constant. It is assumed that there exists the upper cut-off parameter Λ (a positive finite number) for the Fourier components of the order-parameter field $\varphi_i(\mathbf{x})$. Namely, the Fourier–transformed Hamiltonian reads

$$\frac{\mathcal{H}}{k_B T} = \sum_{i,\mathbf{k}} \left(r_0 + c\,\mathbf{k}^2 \right) | \varphi_{i,\mathbf{k}} |^2 + uV^{-1} \sum_{i,j,\mathbf{k}_1,\mathbf{k}_2,\mathbf{k}_3} \varphi_{i,\mathbf{k}_1} \varphi_{i,\mathbf{k}_2} \varphi_{j,\mathbf{k}_3} \varphi_{j,-\mathbf{k}_1-\mathbf{k}_2-\mathbf{k}_3} \,, \tag{2}$$

where $\varphi_{i,\mathbf{k}} = V^{-1/2} \int \varphi_i(\mathbf{x}) \exp(-i\mathbf{k}\mathbf{x}) \, d\mathbf{x}$ and $\varphi_i(\mathbf{x}) = V^{-1/2} \sum_{k < \Lambda} \varphi_{i,\mathbf{k}} \exp(i\mathbf{k}\mathbf{x})$. Moreover, the only allowed configurations of $\varphi_i(\mathbf{x})$ are those, for which $\varphi_{i,\mathbf{k}} = 0$ holds at $k \equiv | \mathbf{k} | > \Lambda$ (therefore we set $\varphi_{i,\mathbf{k}} = 0$ at $k > \Lambda$ in (2)). This is the limiting case $m \to \infty$ of the model where all configurations are allowed, but Hamiltonian (2) is completed by the term $\sum_{i,\mathbf{k}} (k/\Lambda)^{2m} | \varphi_{i,\mathbf{k}} |^2$.

We define the temperature–dependence of the Hamiltonian parameters in vicinity of the critical temperature T_c by a linear relation

$$r_0 = r_{0c} + a(T - T_c) \,, \tag{3}$$

where r_{0c} is the critical value of r_0 and a is a constant. The parameters c and u are assumed to be T–independent. For simplicity, we will consider only the case $T > T_c$ (or $r_0 > r_{0c}$).

2

Using (1) or (2), we can easily calculate the derivative

$$\frac{\partial}{\partial r_0}\left(\frac{F}{k_B T}\right) = -\frac{\partial \ln Z}{\partial r_0} = V \left\langle \varphi^2(\mathbf{x})\right\rangle = n \sum_{k<\Lambda} G(\mathbf{k}) , \tag{4}$$

where $F = -k_B T \ln Z$ is the free energy, $Z = \int \exp[-H/(k_B T)]\mathcal{D}\varphi$ is the partition function and $G(\mathbf{k}) = \langle | \varphi_{i,\mathbf{k}} |^2 \rangle$ (for any $i = 1, 2, \ldots, n$) is the Fourier–transformed two–point correlation function. In the thermodynamic limit at $T > T_c$, the sum over $\mathbf{k}$ in (4) is replaced by the integral according to the well known rule $\sum_{\mathbf{k}} \to V(2\pi)^{-d}\int d\mathbf{k}$ (the term with $\mathbf{k} = \mathbf{0}$ has to be separated at $T < T_c$), where d is the spatial dimensionality. The internal energy $U = -T^2\left(\partial(F/T)/\partial T\right)_V$, calculated from (3) and (4), therefore is

$$U = -a k_B T^2 n V(2\pi)^{-d} \int_{k<\Lambda} G(\mathbf{k})d\mathbf{k} . \tag{5}$$

Consider now the singularity of U and the related singularity of specific heat C_V in vicinity of the critical point at $t \to 0$, where $t = (T - T_c)/T_c$ is the reduced temperature. We assume that the singular part of C_V has the form $\propto (\ln t)^s t^{-\alpha}$ at $t \to 0$. According to the thermodynamic relation $C_V = (\partial U/\partial T)_V$, the corresponding singular part of U is $\propto (\ln t)^s t^{1-\alpha}$ at $t \to 0$. Further on, we will consider the normalized quantities U/V and C_V/V and represent the singularities in terms of the correlation length ξ, assuming the power–law scaling $\xi \propto t^{-\nu}$ at $t \to 0$. The latter is known to be true for the φ^4 model in three dimensions at any $n \geq 1$, as well as at $d = 2$ and $n = 1$. The above relations imply $C_V^{sing} \propto \xi^{1/\nu} U^{sing}$, where U^{sing} and C_V^{sing} are the leading singular parts of U/V and C_V/V, represented in powers of ξ and $\ln \xi$ at $\xi \to \infty$. Using (5), it yields

$$C_V^{sing} = B\xi^{1/\nu}\left(\int_{k<\Lambda}[G(\mathbf{k}) - G^*(\mathbf{k})]d\mathbf{k}\right)^{sing} , \tag{6}$$

where $G^*(\mathbf{k})$ is the value of $G(\mathbf{k})$ at the critical point and B is a nonzero constant. The superscript "$sing$" implies the leading singular contribution in terms of ξ. Since the singular part does not include a constant contribution, it is subtracted in brackets of (6).

Let us denote by $C_V^{sing}(\Lambda')$ the contribution of the integration region $0 < k < \Lambda'$ to (6), where $0 < \Lambda' \leq \Lambda$. Note that $G(\mathbf{k})$ and $G^*(\mathbf{k})$ always correspond to the true upper cut-off Λ. Based on the idea that the short–wavelength contribution is irrelevant, it has been assumed in [8] that $C_V^{sing}(\Lambda')$ is independent of Λ'. To the contrary, here we allow that the amplitude of the leading singularity depends on Λ'. Namely, it is assumed that $C_V^{sing}(\Lambda') = A(\Lambda')(\ln \xi)^\lambda \xi^{\alpha/\nu}$ holds with $\lambda = 0$ corresponding to the usual power–law scaling. In addition, we assume that $\lim_{\Lambda' \to 0} A(\Lambda') \neq 0$ holds, implying that the long–wavelength (small k) contribution to the integral in (6) is relevant. Note that the amplitude $A(\Lambda')$ is determined, considering the limit $\xi \to \infty$ at a fixed Λ'. It means that, even at $\Lambda' \to 0$, the limit $\xi \to \infty$ is considered first and, therefore, the relevant region of small wave vectors $k \sim 1/\xi$ is always included. The above mentioned assumptions have been tested numerically in Sec. 5, clearly showing that they hold in the 2D model with Λ'–dependent amplitude $A(\Lambda')$.

Since we consider the limit $\Lambda' \to 0$, it is naturally to use the scaling hypothesis for the correlation function, which is valid for small k and large ξ. Namely, we have

$$G(\mathbf{k}) = \sum_{i\geq 0}\xi^{(\gamma-\theta_i)/\nu}g_i(k\xi) , \tag{7}$$

3

where $g_i(k\xi)$ are continuous scaling functions, which are finite for $0 \leq k\xi < \infty$. Here $\theta_0 = 0$ holds and the term with $i = 0$ describes the leading singularity, whereas the terms with $i \geq 1$ represent other contributions with correction exponents $\theta_i > 0$. The critical correlation function

$$G^*(\mathbf{k}) = \sum_{i \geq 0} b_i k^{(-\gamma+\theta_i)/\nu} \tag{8}$$

is obtained at $\xi \to \infty$, so that there exists a finite limit

$$\lim_{z \to \infty} z^{(\gamma-\theta_i)/\nu} g_i(z) = b_i , \tag{9}$$

where b_i are constant coefficients. We allow that some of these coefficients are zero. Since we consider only the leading singularity of C_V and the small–k contribution, it is also naturally to assume that only a finite number of correction terms is relevant in our calculations. The assumed validity of (7) and (8) implies that the values of the exponents ensure the convergence of the integral (6) at zero lower integration limit. It means that $d - \gamma/\nu > 0$ must hold at $\theta_i \geq 0$.

Based on the discussed here scaling assumptions, we have obtained an important and challenging result for correction–to–scaling exponents by proving the following theorem.

Theorem. *If the leading singular part of specific heat C_V^{sing} (6) has the form $C_V^{sing} \propto (\ln \xi)^\lambda \xi^{\alpha/\nu}$ and the contribution of the region $k < \Lambda'$ has the form $C_V^{sing}(\Lambda') = A(\Lambda') (\ln \xi)^\lambda \xi^{\alpha/\nu}$ with $\lim_{\Lambda' \to 0} A(\Lambda') \neq 0$, if correct result in the $\lim_{\Lambda' \to 0} \lim_{\xi \to \infty}$ limit (considering $\xi \to \infty$ at a fixed Λ' first) is obtained using (7) –(8) (at the conditions of validity $d - \gamma/\nu > 0$ and $\theta_i \geq 0$, $g_i(z)$ being continuous and finite for $0 \leq z < \infty$ and $\lim_{z \to \infty} z^{(\gamma-\theta_i)/\nu} g_i(z)$ being finite with a large enough finite number of terms included), and if $\gamma + 1 - \alpha - d\nu > 0$ holds, then*

1. *$\lim_{\Lambda' \to 0} | A(\Lambda') | \neq \infty$;*

2. *the two–point correlation function contains a correction–to–scaling term with exponent*

$$\theta_\ell = \gamma + 1 - \alpha - d\nu , \tag{10}$$

   corresponding to a certain term with $i = \ell \geq 1$ in (7).

Proof. Since the correlation function in (7) – (8) is isotropic, $C_V^{sing}(\Lambda')$ can be written as

$$C_V^{sing}(\Lambda') = B\, S(d)\, \xi^{1/\nu} \left(\int\limits_0^{\Lambda'} \sum_{i \geq 0} \left[\xi^{(\gamma-\theta_i)/\nu} g_i(k\xi) - b_i k^{(-\gamma+\theta_i)/\nu} \right] k^{d-1} dk \right)^{sing} , \tag{11}$$

where $S(d) = 2\pi^{d/2}/\Gamma(d/2)$ is the surface of unit sphere in d dimensions. For any finite number of summation terms included, the integration and summation can be exchanged, since the integral exists and converges for each of the terms separately, according to the conditions of validity and properties of scaling functions, mentioned in the theorem, and the fact that Λ' is finite. Then, changing the integration variable to $y = k\xi$, we obtain

$$C_V^{sing}(\Lambda') = B\, S(d) \left(\sum_{i \geq 0} \xi^{-d+(1+\gamma-\theta_i)/\nu} F_i(\Lambda'\xi) \right)^{sing} , \tag{12}$$

4

where

$$F_i(z) = \int_0^z y^{d-1} \widetilde{g}_i(y) dy \qquad \text{with} \quad \widetilde{g}_i(y) = g_i(y) - b_i y^{(-\gamma+\theta_\ell)/\nu} . \tag{13}$$

First we will prove that only one term in (12) gives the leading singular contribution in the limit $\lim_{\Lambda' \to 0} \lim_{\xi \to \infty}$. Since $C_V^{sing}(\Lambda') \propto (\ln \xi)^\lambda \xi^{\alpha/\nu}$ holds, only those terms can give the leading singularity at $\xi \to \infty$, which are proportional to $(\ln \xi)^\lambda \xi^{\alpha/\nu}$ in this limit. It implies that

$$F_i(\Lambda'\xi) \propto \left[\ln(\Lambda'\xi) \right]^\lambda (\Lambda'\xi)^{\mu_i} \tag{14}$$

must hold for these terms at $\Lambda'\xi \to \infty$ with

$$-d + (1+\gamma-\theta_i)/\nu + \mu_i = \alpha/\nu , \quad i \in \Omega . \tag{15}$$

Here Ω is the subset of indices i, labeling these terms. According to the conditions of the theorem, Ω contains a finite number of indices. If there exist several terms with $i \in \Omega$, then they all have different exponents μ_i because θ_i in (15) are different by definition. In the limit $\lim_{\Lambda' \to 0} \lim_{\xi \to \infty}$, these terms give contributions $\propto (\Lambda')^{\mu_i} (\ln \xi)^\lambda \xi^{\alpha/\nu}$, as consistent with (12) and (14) – (15). Consequently, at $\Lambda' \to 0$, the amplitude is

$$A(\Lambda') \propto (\Lambda')^{\mu_\ell} , \tag{16}$$

where $\mu_\ell = \min_{i \in \Omega} \mu_i$. Thus, we have proven the statement that only one of the terms in (12) with certain index $i = \ell$ gives the leading singularity at $\lim_{\Lambda' \to 0} \lim_{\xi \to \infty}$. This is not necessarily the leading term with $\ell = 0$, since the integration over k can give a vanishing result due to the cancellation of positive and negative contributions. Formally, there is also a possibility that some terms give analytic contributions, which are constant or proportional to an integer power of t (integer power of $\xi^{-1/\nu}$). By definition, such terms are considered as non-singular and not contributing to $C_V^{sing}(\Lambda')$.

In the following we will prove the statement $\lim_{\Lambda' \to 0} | A(\Lambda') | \neq \infty$ by assuming the opposite and deriving a contradiction. Thus, let us assume that $A(\Lambda')$ diverges at $\Lambda' \to 0$. According to (16), it is possible only for $\mu_\ell < 0$. Hence, from (13) and (14) we find that

$$F_\ell(z) = \int_0^z y^{d-1} \widetilde{g}_\ell(y) dy = c_\ell (\ln z)^\lambda z^{\mu_\ell} \tag{17}$$

holds at $\mu_\ell < 0$ for large $z = \Lambda'\xi \to \infty$, corresponding to the considered here limit $\lim_{\Lambda' \to 0} \lim_{\xi \to \infty}$. Here c_ℓ is a nonzero constant, and (17) holds asymptotically with relative error tending to zero at $z \to \infty$. The derivation with respect to z in (17) yields

$$\widetilde{g}_\ell(z) = c_\ell \left[\lambda(\ln y)^{-1} + \mu_\ell \right] (\ln z)^\lambda z^{\mu_\ell - d} \qquad \text{at} \quad z \to \infty . \tag{18}$$

Consequently, the integrand function with $i = \ell$ in (13), i. e., $f(y) = y^{d-1} \widetilde{g}_\ell(y)$, converges to $f_{as}(y)$ at $y \to \infty$ in such a way that $(f(y) - f_{as}(y))/f_{as}(y) \to 0$, where

$$f_{as}(y) = c_\ell \left[\lambda(\ln y)^{-1} + \mu_\ell \right] (\ln y)^\lambda y^{\mu_\ell - 1} \tag{19}$$

is the asymptotic form of $f(y)$. It implies that, for any given finite $\varepsilon > 0$, there exists a finite $y_0 > 0$, such that $| f(y) - f_{as}(y) | / | f_{as}(y) | < \varepsilon$ holds for $y > y_0$. Since $| f(y) | - | f_{as}(y) | \leq | f(y) - f_{as}(y) |$ always holds, we have also

$$\frac{| f(y) | - | f_{as}(y) |}{| f_{as}(y) |} < \varepsilon \qquad \text{for} \quad y > y_0 . \tag{20}$$

At this condition, the integral (13) with $i = \ell$ converges at $z \to \infty$. To prove this statement, the integral at $z \to \infty$ is written as $\int_0^\infty f(y) dy = \int_0^{y_0} f(y) dy + \int_{y_0}^\infty f(y) dy$. The first integral $\int_0^{y_0} f(y) dy$ exists and it has a finite value because the scaling function $g_\ell(y)$ is continuous and finite within $0 \le y \le y_0$, as well as $d - \gamma/\nu > 0$ and $\theta_\ell \ge 0$ hold for the exponents. Using (20), the second integral can be evaluated as

$$\left| \int_{y_0}^\infty f(y) dy \right| \le \int_{y_0}^\infty |f(y)| \, dy < \int_{y_0}^\infty |f_{as}(y)| \, (1 + \varepsilon) dy . \tag{21}$$

The latter integral in (21) converges according to (19), since $\mu_\ell < 0$ holds. Consequently, the integral $\lim_{z \to \infty} F_\ell(z) = \int_0^\infty f(y) dy$ also converges. It means that $F_\ell(z)$ tends to a constant at $z \to \infty$ and, according to (12), the amplitude $A(\Lambda')$ is constant at $\Lambda' \to 0$. It contradicts the initial assumption that $A(\Lambda')$ diverges at $\Lambda' \to 0$, so that this assumption is false, i. e., $\lim_{\Lambda' \to 0} |A(\Lambda')| \ne \infty$.

Finally, we will prove the relation (10). Since $\lim_{\Lambda' \to 0} A(\Lambda') \ne 0$ holds according to the conditions of the theorem, we have $\mu_\ell \le 0$ in (16). On the other hand, since $\lim_{\Lambda' \to 0} |A(\Lambda')| \ne \infty$, we have $\mu_\ell \ge 0$. Consequently, $\mu_\ell = 0$ holds. Eq. (15) with $i = \ell \in \Omega$ then leads to (10). The condition $\gamma + 1 - \alpha - d\nu > 0$ of the theorem implies that (10) is satisfied with $\theta_\ell > 0$, which corresponds to a correction term with $i = \ell > 0$ in (7) (the term with $i = 0$ gives no contribution to $C_V^{sing}(\Lambda')$ at $\lim_{\Lambda' \to 0} \lim_{\xi \to \infty}$). $\square$

One has to note that, according to the self–consistent scaling theory of logarithmic correction exponents in [12], logarithmic corrections can generally appear in ξ as function of t, as well as in $G(\mathbf{k})$. Nevertheless, our consideration covers the usual case of $\lambda = 0$, where no logarithmic corrections are present, as well as the important particular case of $\alpha = 0$ and $\lambda = 1$, where the logarithmic correction appears only in specific heat [12]. The considered here scaling forms appear to be general enough for our analysis of the φ^4 model below the upper critical dimension $d < 4$, where ξ and $G(\mathbf{k})$ have no logarithmic corrections according to the known results, except only for the case of the Kosterlitz–Thouless phase transition at $n = 2$ and $d = 2$. According to the current knowledge about the critical phenomena, the used here scaling forms, as well as the assumed relations for the exponents $d - \gamma/\nu > 0$ and $\gamma + 1 - \alpha - d\nu > 0$ hold for $d = 3$, $n \ge 1$ and also for $d = 2$, $n = 1$. The other conditions of the theorem are satisfied in these cases, according to the provided here general arguments and numerical tests in Sec. 5.

The existence of a correction with exponent $\theta_\ell = 3/4$ in the scalar ($n = 1$) 2D φ^4 model follows from this theorem, if $\gamma = 7/4$ and $\nu = 1$ hold here, as in the 2D Ising model. It corresponds to a correction exponent $\omega_\ell = \theta_\ell/\nu = 3/4$ in the critical two–point correlation function, as well as in the finite–size scaling. Since this exponent not necessarily describes the leading correction term, the prediction is $\omega \le 3/4$ for the leading correction–to–scaling exponent ω. An evidence for a nontrivial correction with non–integer exponent (which might be, e. g., 1/4) in the finite–size scaling of the critical real–space two–point correlation function of the 2D Ising model has been provided in [13], based on an exact enumeration by a transfer matrix algorithm. This correction, however, has a very small amplitude and is hardly detectable. Moreover, such a correction has not been detected in susceptibility. Usually, the scaling in the 2D Ising model is representable by trivial, i. e., integer, correction–to–scaling exponents when analytical background terms or "short–distance" terms (e. g., a constant contribution to susceptibility) are separated

– see, e. g., [14–16] and references therein. The discussions have been focused on the existence of irrelevant variables [17, 18]. In particular, the high–precision calculations in [18] have shown that the conjecture by Aharony and Fisher about the absence of such variables [19, 20] fails.

The above mentioned theorem predicts the existence of nontrivial correction–to–scaling exponents in the 2D φ^4 model. It can be expected that the nontrivial correction terms of the φ^4 model usually do not show up or cancel in the 2D Ising model. This idea is not new. Based on the standard field–theoretical treatments of the φ^4 model, $\omega = 4/3$ has been conjectured for the leading nontrivial scaling corrections at $n = 1$ and $d = 2$ in [3, 21]. However, it contradicts our theorem, which yields $\omega \le 3/4$. This discrepancy is interpreted as a failure of the standard perturbative methods — see [7] and the discussions in [8]. One has to note that the alternative perturbative approach of [6], predicting $\omega_\ell = \ell\eta$ (where $\ell \ge 1$ is an integer) with $\eta = 2 - \gamma/\nu = 1/4$ for $n = 1$ and $d = 2$, is consistent with this theorem.

3 Monte Carlo simulation of the lattice φ^4 model

We have performed MC simulations of the scalar 2D φ^4 model on square lattice with periodic boundary conditions. The Hamiltonian $\mathcal{H}$ is given by

$$\frac{\mathcal{H}}{k_B T} = -\beta \sum_{\langle ij \rangle} \varphi_i \varphi_j + \sum_i \left(\varphi_i^2 + \lambda \left(\varphi_i^2 - 1 \right)^2 \right) , \tag{22}$$

where $-\infty < \varphi_i < \infty$ is a continuous scalar order parameter at the i-th lattice site, and $\langle ij \rangle$ denotes the set of all nearest neighbors. This notation is related to the one of [22] via $\beta = 2\kappa$ and $\varphi = \phi$. We have denoted the coupling constant at $\varphi_i \varphi_j$ by β to outline the similarity with the Ising model.

Swendsen-Wang and Wolff cluster algorithms are known to be very efficient for MC simulations of the Ising model in vicinity of the critical point [23]. However, these algorithms update only the spin orientation, and therefore are not ergodic for the φ^4 model. The problem is solved using the hybrid algorithm, where a cluster algorithm is combined with Metropolis sweeps. This method has been applied to the 3D φ^4 model in [22]. In our simulations, we have applied one Metropolis sweep after each N_W Wolff single cluster algorithm steps. Following [22], a new value of the order parameter is chosen as $\varphi_i' = \varphi_i + s(r - 1/2)$ in one Metropolis step (this value being either accepted or rejected, as usually) where s is a constant and r is a random number from a set of uniformly distributed random numbers within $[0, 1]$. Here N_W and s are considered as optimization parameters, allowing to reach the smallest statistical error in a given simulation time. We have chosen N_W such that $N_W \langle c \rangle / L^2$ is about $2/3$ or 0.6, where $\langle c \rangle$ is the mean cluster size. The optimal choice of s depends on the Hamiltonian parameters. Our simulations have been performed at $\lambda = 0.1$, $\lambda = 1$, $\lambda = 10$ and at such values of β, which correspond to $U = \langle m^4 \rangle / \langle m^2 \rangle^2 = 1.1679229 \approx U^*$ and $U = 2$, m being the magnetization per spin. Here U^* is the λ–independent (universal) critical value of U, which has been evaluated as $U^* = 1.1679229 \pm 0.0000047$ in [17]. At $U = 1.1679229$, we have chosen $s = 4$ for $\lambda = 0.1$, $s = 4$ for $\lambda = 1$ and $s = 3$ for $\lambda = 10$. At $U = 2$, the corresponding values are $s = 3.5$, $s = 3$ and $s = 2$. For comparison, $s = 3$ has been used in [22].

We have used the iterative method of [24] to find β, corresponding to certain value of U, as well as a set of statistical averaged quantities at this β, called the pseudo-critical

coupling $\widetilde{\beta}_c(L)$. We have performed high statistics simulations for evaluation of the derivative $\partial U/\partial\beta$ and the susceptibility $\chi = N\langle m^2\rangle$, where $N = L^2$ is the total number of spins. According to the Boltzmann statistics, the derivative with respect to β for any quantity $\langle\mathcal{A}\rangle$ is calculated as

$$\frac{\partial}{\partial\beta}\langle\mathcal{A}\rangle = N\left[\langle\mathcal{A}\rangle\langle\varepsilon\rangle - \langle\mathcal{A}\varepsilon\rangle\right] , \qquad (23)$$

where $\varepsilon = -N^{-1}\sum_{\langle ij\rangle}\varphi_i\varphi_j$.

For each lattice size L, the quantities χ and $\partial U/\partial\beta$ have been estimated from 100 iterations (simulation bins) in vicinity of $\beta = \widetilde{\beta}_c(L)$, collected from one or several simulation runs, discarding first 10 iterations of each run for equilibration. One iteration included 10^6 steps of the hybrid algorithm, each consisting of one Metropolis sweep and N_W Wolff algorithm steps, as explained before. To test the accuracy of our iterative method, we have performed some simulations (for $U = 2$ and $\lambda = 0.1$) with 2.5×10^5 hybrid algorithm steps in one iteration, and have verified that the results well agree with those for 10^6 steps. Moreover, we have used two different pseudo-random number generators, the same ones as in [25], to verify that the results agree within the statistical error bars.

Note that the quantity U is related to the Binder cumulant $B = 1 - U/3$ [9]. In the thermodynamic limit, we have $B = 0$ ($U = 3$) above the critical point, i. e., at $T > T_c$ or $\beta < \beta_c$, and $B = 2/3$ ($U = 1$) at $T < T_c$ or $\beta > \beta_c$. Thus, the pseudo-critical coupling $\widetilde{\beta}_c(L)$, corresponding to a given U in the range of $1 < U < 3$, tends to the true critical coupling β_c at $L \to \infty$. The iterative algorithm of [24] is valid for any $1 < U < 3$. However, it can be useful to choose $U \approx U^*$ for MC analysis. In particular, it allows us to obtain $\widetilde{\beta}_c(L)$ values closer to the true critical coupling β_c. On the other hand, it is crucial for our MC analysis in Sec. 6 to have the data for at least two remarkably different values of U. Therefore, we have chosen one U value, $U = 2$, in the middle of the interval $1 < U < 3$ and the other one, $U = 1.1679229$, close to the critical value U^* at $\beta = \beta_c$ and $L \to \infty$.

MC simulations have been performed for lattice sizes $4 \le L \le L_{\max}$ whith $L_{\max} = 256$ at $\lambda = 10$, $L_{\max} = 384$ at $\lambda = 1$ and $L_{\max} = 1536$ at $\lambda = 0.1$. This choice of $L_{\max}$ is motivated by the fact that at $\lambda = 0.1$ we have observed an interesting scaling behavior and, therefore, the simulations have been extended up to $L = 1536$ for a refined analysis.

In addition, we have performed some simulations with the hybrid algorithm at certain fixed values of the reduced temperature $t = 1 - \beta/\beta_c$ and have evaluated the Fourier–transformed two–point correlation function $G(\mathbf{k})$ and its derivative $\partial G(\mathbf{k})/\partial\beta$ in order to test the conditions of the theorem in Sec. 2. These results are discussed in Sec. 5.

A parallel algorithm, similar to that one used in [24], helped us to speed up the simulations. The Wolff algorithm has been parallelized in this way, whereas the usual ideas of splitting the lattice in slices [23] have been applied to parallelize the Metropolis algorithm. In the current application, the parallel code showed a quite good scalability (for Wolff, as well as Metropolis, algorithms) up to 8 processors available on one node of the cluster. The simulation results for χ and $\partial U/\partial\beta$ are collected in Tabs. 1 to 6.

4   Estimation of the critical coupling

According to the finite–size scaling theory, U behaves asymptotically as $U = F\left((\beta - \beta_c)L^{1/\nu}\right)$ (see, e. g., the references in [22]) for large lattice sizes in vicinity of the critical point, where $F(z)$ is a smooth function of z. Hence, the pseudo-critical

Table 1: The values of $\widetilde{\beta}_c$, as well as $\chi/L^{7/4}$, and $-(\partial U/\partial \beta)/L$ at $\beta = \widetilde{\beta}_c$ for $\lambda = 0.1$ and $U = 2$ depending on the lattice size L.

L	$\widetilde{\beta}_c$	$\chi/L^{7/4}$	$-(\partial U/\partial \beta)/L$
4	0.549398(42)	0.60791(23)	2.4344(16)
6	0.562326(28)	0.50107(21)	2.5045(17)
8	0.570550(19)	0.44694(19)	2.5492(21)
12	0.580455(14)	0.39460(21)	2.5900(22)
16	0.5861408(94)	0.36991(17)	2.6112(26)
24	0.5924039(62)	0.34936(16)	2.6459(26)
32	0.5957584(45)	0.34116(15)	2.6663(30)
48	0.5992406(34)	0.33538(14)	2.6881(27)
64	0.6010332(23)	0.33412(13)	2.7129(31)
96	0.6028383(15)	0.33359(14)	2.7273(36)
128	0.6037470(11)	0.33396(14)	2.7351(40)
192	0.60465804(69)	0.33486(14)	2.7592(37)
256	0.60511333(60)	0.33537(12)	2.7614(38)
384	0.60556996(40)	0.33648(12)	2.7745(38)
512	0.60579773(41)	0.33701(11)	2.7780(40)
768	0.60602518(20)	0.337618(99)	2.7836(37)
1024	0.60613849(13)	0.33780(13)	2.7827(44)
1536	0.606252278(88)	0.33825(11)	2.7890(40)

Table 2: The same quantities as in Tab. 1 for $\lambda = 0.1$ and $U = 1.1679229 \approx U^*$.

L	$\widetilde{\beta}_c$	$\chi/L^{7/4}$	$-(\partial U/\partial \beta)/L$
4	0.657515(35)	2.34779(47)	0.80400(54)
6	0.631043(25)	1.92047(42)	0.86944(59)
8	0.620578(18)	1.70494(34)	0.91842(62)
12	0.612621(12)	1.49436(34)	0.98840(78)
16	0.6097815(87)	1.39473(29)	1.03343(72)
24	0.6077860(60)	1.30274(25)	1.08458(88)
32	0.6071398(45)	1.26197(23)	1.11290(88)
48	0.6067318(29)	1.22651(20)	1.1405(10)
64	0.6065998(21)	1.21076(20)	1.1527(10)
96	0.6065241(13)	1.19834(18)	1.1662(11)
128	0.60649879(98)	1.19250(16)	1.1691(12)
192	0.60648734(65)	1.18840(17)	1.1773(12)
256	0.60648276(42)	1.18684(16)	1.1821(12)
384	0.60648026(37)	1.18525(16)	1.1827(13)
512	0.60647976(24)	1.18469(14)	1.1826(13)
768	0.60647922(16)	1.18400(15)	1.1824(13)
1024	0.60647921(13)	1.18389(15)	1.1822(15)
1536	0.606479145(90)	1.18358(14)	1.1814(15)

Table 3: The same quantities as in Tab. 1 for $\lambda = 1$ and $U = 2$.

L	$\widetilde{\beta}_c$	$\chi/L^{7/4}$	$-(\partial U/\partial \beta)/L$
4	0.512944(44)	0.315623(68)	1.27395(46)
6	0.562964(29)	0.285305(62)	1.26851(65)
8	0.590002(23)	0.270748(70)	1.26492(60)
12	0.618562(16)	0.257116(64)	1.25903(71)
16	0.633498(12)	0.251359(59)	1.25682(77)
24	0.6488801(88)	0.246529(69)	1.25454(83)
32	0.6567123(57)	0.244758(59)	1.25660(94)
48	0.6646251(41)	0.243446(55)	1.25736(90)
64	0.6686081(32)	0.243132(52)	1.26232(87)
96	0.6726031(19)	0.242971(54)	1.26114(90)
128	0.6745993(15)	0.242899(53)	1.2624(10)
192	0.6766057(11)	0.243177(58)	1.2653(12)
256	0.67760534(71)	0.243253(50)	1.26330(93)
384	0.67860417(52)	0.243323(53)	1.26412(99)

Table 4: The same quantities as in Tab. 1 for $\lambda = 1$ and $U = 1.1679229 \approx U^*$.

L	$\widetilde{\beta}_c$	$\chi/L^{7/4}$	$-(\partial U/\partial \beta)/L$
4	0.722627(50)	1.04218(11)	0.42994(15)
6	0.697790(35)	0.968521(95)	0.46880(16)
8	0.689603(26)	0.932407(93)	0.48802(19)
12	0.684134(15)	0.898059(93)	0.50719(22)
16	0.682362(13)	0.88219(11)	0.51584(28)
24	0.6812691(70)	0.868287(84)	0.52464(27)
32	0.6809349(57)	0.862141(79)	0.52862(24)
48	0.6807164(37)	0.856758(66)	0.53201(25)
64	0.6806597(26)	0.854718(69)	0.53383(30)
96	0.6806247(19)	0.852876(74)	0.53536(33)
128	0.6806146(16)	0.851979(80)	0.53527(36)
192	0.68060666(96)	0.851343(62)	0.53597(34)
256	0.68060766(79)	0.851228(63)	0.53655(37)
384	0.68060481(50)	0.850877(85)	0.53608(44)

Table 5: The same quantities as in Tab. 1 for $\lambda = 10$ and $U = 2$.

L	$\widetilde{\beta}_c$	$\chi/L^{7/4}$	$-(\partial U/\partial \beta)/L$
4	0.287517(24)	0.367807(43)	1.53677(43)
8	0.374876(16)	0.332360(53)	1.35076(57)
16	0.4217519(94)	0.314668(54)	1.27009(55)
32	0.4461113(40)	0.305725(47)	1.23283(56)
64	0.4585487(24)	0.301387(50)	1.21446(69)
128	0.4648281(11)	0.299070(47)	1.20451(70)
256	0.46798547(75)	0.297843(55)	1.19889(89)

Table 6: The same quantities as in Tab. 1 for $\lambda = 10$ and $U = 1.1679229 \approx U^*$.

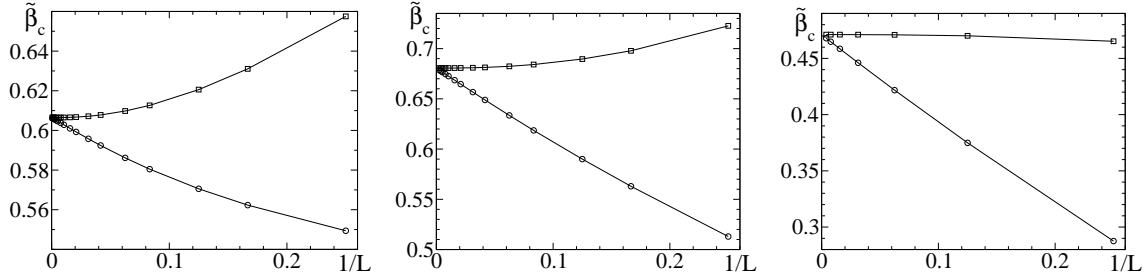| L	$\widetilde{\beta}_c$	$\chi/L^{7/4}$	$-(\partial U/\partial \beta)/L$
4	0.465260(24)	1.005811(34)	0.532729(66)
8	0.470103(15)	1.025510(55)	0.51648(13)
16	0.4709851(82)	1.032848(67)	0.50965(18)
32	0.4711260(32)	1.035132(50)	0.50721(14)
64	0.4711546(20)	1.036045(62)	0.50704(20)
128	0.4711559(11)	1.036188(67)	0.50673(23)
256	0.47115644(49)	1.036266(58)	0.50653(21)

Figure 1: The pseudo-critical coupling $\widetilde{\beta}_c$ vs $1/L$ for $\lambda = 0.1$ (left), $\lambda = 1$ (middle) and $\lambda = 10$ (right). The upper plots (squares) and the lower plots (circles) refer to the cases $U = 1.1679229 \approx U^*$ and $U = 2$, respectively. Statistical errors are much smaller than the symbol size.

coupling $\widetilde{\beta}_c$ behaves as

$$\widetilde{\beta}_c = \beta_c + aL^{-1/\nu} \qquad (24)$$

at large L, where the coefficient a depends on U and λ. Since $\nu = 1$ holds in this model, it is meaningful to plot $\widetilde{\beta}_c$ vs $1/L$ as it is done in Fig. 1.

At the critical U value, $U = U^*$, the coefficient a vanishes and the asymptotic convergence of $\widetilde{\beta}_c$ to the critical coupling β_c is faster than $\sim 1/L$. As one can judge from Fig. 1, it occurs at $U = 1.1679229 \approx U^*$ for all λ. In this sense U^* is universal. The estimate $U^* = 1.1679229 \pm 0.0000047$ has been obtained in [17] for the 2D Ising model, corresponding to the limit $\lambda \to \infty$.

The critical coupling β_c can be evaluated by fitting the $\widetilde{\beta}_c$ data at $U = 2$ to the ansatz (24). Alternatively, the data for $U = 1.1679229 \approx U^*$ can be used. The coefficient a in (24) vanishes at $U = U^*$ and the convergence to β_c is very fast in this case. Therefore, the value of $\widetilde{\beta}_c(L)$ at the maximal lattice size $L = L_{\max}$ for $U = 1.1679229$ can be assumed as a reasonable estimate of β_c, and $\pm \mid \widetilde{\beta}_c(L_{\max}) - \widetilde{\beta}_c(L_{\max}/2) \mid$ can be assumed as error bars for the systematical errors. One has to take into account also the statistical errors in $\widetilde{\beta}_c(L_{\max})$ and $\mid \widetilde{\beta}_c(L_{\max}) - \widetilde{\beta}_c(L_{\max}/2) \mid$. The estimates $\beta_c = 0.60647915 \pm 0.00000035$ at $\lambda = 0.1$, $\beta_c = 0.680605 \pm 0.000004$ at $\lambda = 1$ and $\beta_c = 0.4711564 \pm 0.0000020$ at $\lambda = 10$ have been obtained by this method.

These estimates well agree with those obtained by fitting the data for $U = 2$ to (24). These fits, however, are somewhat problematic, since it is not possible to fit reasonably well more than three data points. Since the data for relatively large lattice sizes are available at $\lambda = 0.1$ and $U = 2$, the problem is resolved by using a refined ansatz

$$\widetilde{\beta}_c = \beta_c + a_1 L^{-1/\nu} + a_2 L^{-\omega - 1/\nu} \ . \qquad (25)$$

Here we set $\nu = 1$, as in the 2D Ising model. If corrections to scaling are such as in the 2D Ising model, then we have $\omega = 1$ in (25). However, according to the analytical arguments in Sec. 2 and our following numerical analysis, smaller values of ω can be expected, such as $3/4$, $1/2$ or even $1/4$. Fortunately, the fits within $L \in [L_{\min}, 1536]$ with $L_{\min} = 192$ are acceptable and the fitted value of β_c is very robust, i. e., it only weakly depends on ω. Namely, we obtain $\beta_c = 0.60647936(24)$ with $\chi^2/\text{d.o.f.} = 1.18$ (where $\chi^2/\text{d.o.f.}$ is the value of χ^2 per degree of freedom of the fit [23, 26]) at $\omega = 1$, $\beta_c = 0.60647915(30)$ with $\chi^2/\text{d.o.f.} = 1.14$ at $\omega = 0.5$, and $\beta_c = 0.60647897(35)$ with $\chi^2/\text{d.o.f.} = 1.15$ at

12

$\omega = 0.25$. Moreover, the fits with $L_{\min} = 256$ well confirm these results. Taking into account the statistical, as well as the systematical errors (due to the uncertainty in ω and influence of $L_{\min}$), our estimate of the critical coupling at $\lambda = 0.1$ by this method is $\beta_c = 0.606479 \pm 0.000001$.

According to (1), the fluctuations of φ_i^2 are suppressed at $\lambda \to \infty$ in such a way that $\varphi_i^2 \to 1$ holds for relevant spin configurations with finite values of $H/(k_B T)$ per spin. It means that the actual φ^4 model becomes equivalent to the Ising model, where $\varphi_i = \pm 1$, in the limit $\lambda \to \infty$, further called the Ising limit. Thus, it is not surprising that β_c approaches the known exact value $\frac{1}{2} \ln \left(1 + \sqrt{2}\right) = 0.44068679\ldots$ of the 2D Ising model [27] when λ becomes large.

It is somewhat unexpected that β_c appears to be a non-monotonous function of λ. It can be explained by two competing effects. On the one hand, fluctuations increase with decreasing of λ, and therefore β_c tends to increase. Indeed, β_c at $\lambda = 1$ is remarkably larger than that at $\lambda = 10$. On the other hand, an effective interaction between spins becomes stronger for small λ because $\langle |\varphi_i| \rangle$ and therefore also $\langle \varphi_i \varphi_j \rangle$ for neighboring spins increases in this case. It can explain the fact that β_c at $\lambda = 0.1$ is slightly smaller than that at $\lambda = 1$.

5 Numerical test of the conditions of the theorem

Let us consider the quantity

$$\Psi = 2\pi \frac{\partial}{\partial \beta} \langle \varphi^2 \rangle = \frac{2\pi}{L^2} \sum_{\mathbf{k}} \frac{\partial}{\partial \beta} G(\mathbf{k}) \tag{26}$$

in the scalar 2D lattice φ^4 model, where $G(\mathbf{k}) = \langle |\varphi_{\mathbf{k}}|^2 \rangle$ with $\varphi_{\mathbf{k}} = L^{-1} \sum_{\mathbf{x}} \varphi(\mathbf{x}) \exp(-i\mathbf{kx})$ is the Fourier–transformed two–point correlation function, and the summation in (26) takes place over wave vectors $\mathbf{k} = (k_x, k_y)$ with components $k_x = 2\pi j/L$ and $k_y = 2\pi l/L$, j and l being integers ranging from $1 - L + [L/2]$ to $[L/2]$, where $[L/2]$ denotes the integer part of $L/2$. In the thermodynamic limit $L \to \infty$ above the critical point ($\beta < \beta_c$), the sum in (26) becomes an integral

$$\Psi = \frac{1}{2\pi} \int\limits_{|k_x|,|k_y| \leq \pi} \frac{\partial}{\partial \beta} G(\mathbf{k}) d\mathbf{k} = -\frac{1}{2\pi \beta_c} \frac{\partial}{\partial t} \int\limits_{|k_x|,|k_y| \leq \pi} G(\mathbf{k}) d\mathbf{k} \tag{27}$$

where $t = 1 - \beta/\beta_c$ is the reduced temperature. The same quantity can be considered in the continuous φ^4 model of Sec. 2 in two dimensions with the only difference that the integration region is $k = \sqrt{k_x^2 + k_y^2} < \Lambda$ and t is defined by (3) there. Moreover, the small-k contributions are similar in both cases, since the correlation function is isotropic at $k \to 0$ in both models. According standard universality arguments, these contributions thus have singularities of the same kind, which are described by the same critical exponents and logarithmic corrections at $t \to 0$. Moreover, according to (5) and $C_V = (\partial U/\partial T)_V$, we have an equivalent to (6) representation of C_V^{sing} in the form of

$$C_V^{sing} \propto \left(\frac{\partial}{\partial t} \int\limits_{k < \Lambda} G(\mathbf{k}) d\mathbf{k} \right)^{sing}, \tag{28}$$

13

so that the small-k contribution to specific heat in the continuous model also has the singularity of this kind. Since $G(\mathbf{k})$ is isotropic at $k \to 0$, the contribution of a small-k region $k < \Lambda' \ll \pi$, denoted as $\Psi(\Lambda')$, can be represented as

$$\Psi(\Lambda') = \int\limits_0^{\Lambda'} k\, \frac{\partial}{\partial\beta} G(k)\, dk = \sum_{0 < k < \Lambda'} k\, \frac{\partial}{\partial\beta} G(k)\, \Delta k \qquad \text{at} \quad \Delta k \to 0 \tag{29}$$

in the thermodynamic limit at $\Lambda' \to 0$, where $G(k)$ is the correlation function in the $\langle 10 \rangle$ crystallographic direction, i. e., at $\mathbf{k} = (k, 0)$ or $\mathbf{k} = (0, k)$, and the summation runs over k values $l\Delta k$ with integer $l > 0$ and $\Delta k = 2\pi/L$.

In the following we consider the quantity

$$\Phi = \sum_{0 < k \le \pi} k\, \frac{\partial}{\partial\beta} G(k)\, \Delta k \;, \tag{30}$$

which has the same small-k contribution as Ψ, but is more convenient for simulations. The small-k contribution can be calculated from

$$\Phi(\Lambda') = \Phi(\pi) - \Delta\Phi(\Lambda') \;, \tag{31}$$

where $\Phi(\pi) \equiv \Phi$ and

$$\Delta\Phi(\Lambda') = \sum_{\Lambda' \le k \le \pi} k\, \frac{\partial}{\partial\beta} G(k)\, \Delta k \;, \tag{32}$$

is the short-wavelength, i. e., large-k contribution.

The correlation function in the $\langle 10 \rangle$ direction is calculated as $\langle |\varphi_{\mathbf{k}}|^2 \rangle$ for $\mathbf{k} = (k, 0)$, i. e.,

$$G(k) = \left\langle L^{-2} \left[\left(\sum_{x=0}^{L-1} \sigma(x) \cos(kx) \right)^2 + \left(\sum_{x=0}^{L-1} \sigma(x) \sin(kx) \right)^2 \right] \right\rangle \;, \tag{33}$$

where $\sigma(x) = \sum_{y=0}^{L-1} \varphi(x,y)$ with $\varphi(x,y) = \varphi(\mathbf{r})$ at $\mathbf{r} = (x, y)$. The result for $\langle 01 \rangle$ direction is obtained by exchanging x and y. We have averaged over both equivalent cases to obtain more accurate values of $G(k)$ from MC simulations. The derivative $\partial G(k)/\partial\beta$ is calculated using (23).

We have performed MC simulations for $\lambda = 0.1$ at certain values of the reduced temperature, $t = 1 - \beta/\beta_c = 0.08, 0.04, 0.02, 0.01, 0.005$, assuming $\beta_c = 0.606479$ in accordance with the estimation in Sec. 4. The error in this β_c value is as small as few times 10^{-7} and therefore is negligible in our analysis. The simulations have been performed for lattice sizes $L = 16, 32, 64, 128, 256, 512, 1024$ and 2048 in order to evaluate the quantities Φ and $\Delta\Phi(\Lambda')$ for $tL = 1.28, 2.56, 5.12$ and 10.24. It corresponds to $L/\xi_{2\mathrm{nd}} \approx 6.9, 13.8, 27.6$ and 55.2 at the largest L values, where $\xi_{2\mathrm{nd}}$ is the second moment correlation length, defined as in [28], i. e., $\xi_{2\mathrm{nd}} = \sqrt{[(\chi/G(2\pi/L)) - 1]/[4\sin^2(\pi/L)]}$. According to this, it can be expected that the results for $tL = 5.12$ and $tL = 10.24$ provide good approximations for the thermodynamic limit, since $L/\xi_{2\mathrm{nd}} \gg 1$ holds. It is confirmed by the Φ vs $\ln t$ plots in Fig. 2 and $\Delta\Phi(\Lambda')$ vs $\ln t$ plots in Fig. 3, showing a fast convergence to the thermodynamic limit with increasing of tL at a fixed t.

These plots tend to become linear at large tL and small t values. It indicates that Φ and $\Delta\Phi(\Lambda')$ have logarithmic singularities in the thermodynamic limit at $t \to 0$. Moreover, it holds for $\Delta\Phi(\Lambda')$ at arbitrary Λ', implying that $\partial G(k)/\partial\beta$ has the logarithmic
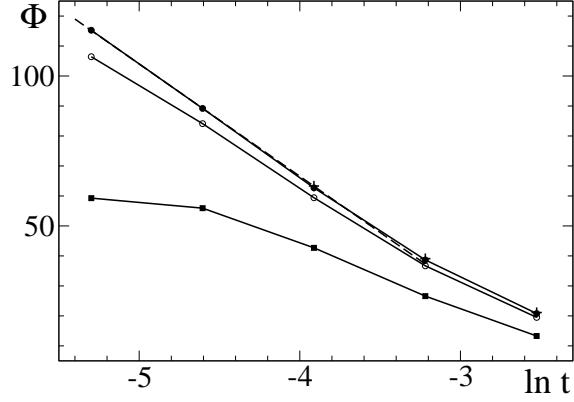
14

Figure 2: The Φ vs $\ln t$ plots at $tL = 1.28$ (squares), $tL = 2.56$ (empty circles), $tL = 5.12$ (solid circles) and $tL = 10.24$ (pluses). The dashed straight line shows that the plot at $tL = 5.12$ is almost linear within $0.005 \leq t \leq 0.04$. Statistical errors are smaller than symbol size.
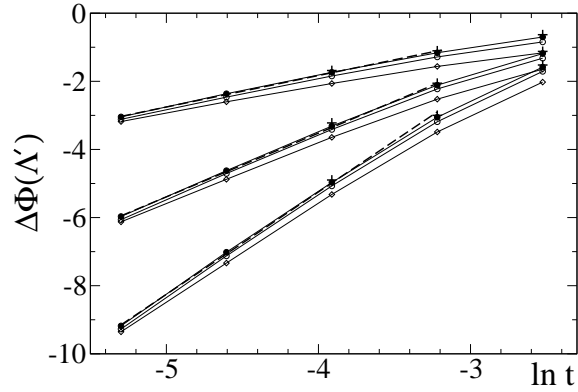

Figure 3: The $\Delta\Phi(\Lambda')$ vs $\ln t$ plots at $tL = 1.28$ (diamonds), $tL = 2.56$ (empty circles), $tL = 5.12$ (solid circles) and $tL = 10.24$ (pluses) for $\Lambda' = 7\pi/8$ (upper plots), $\Lambda' = 3\pi/4$ (middle plots) and $\Lambda' = 5\pi/8$ (lower plots). The dashed straight lines are depicted to show that the plots at $tL = 5.12$ are almost linear for small t values. Statistical errors are smaller than symbol size.

15
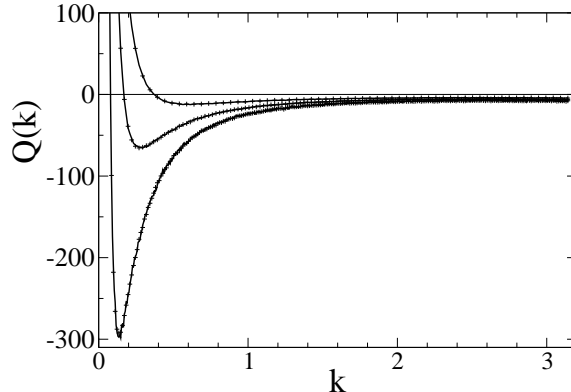
Figure 4: $Q(k) = k \, \partial G(k)/\partial\beta$ vs k plots at $t = 0.02$ (upper curve), $t = 0.01$ (middle curve) and $t = 0.005$ (lower curve). The results for $tL = 5.12$ are shown by curves, whereas those for $tL = 2.56$ – by pluses. The pluses lie practically on the top of curves, showing that the thermodynamic limit is reached with a high accuracy at $tL = 5.12$.

singularity at $t \to 0$ for any fixed non-zero k in the thermodynamic limit. Although we have tested only the $\langle 10 \rangle$ direction, this, obviously, is true also for $\partial G(\mathbf{k})/\partial\beta$ and $\partial G(\mathbf{k})/\partial t = -\beta_c \partial G(\mathbf{k})/\partial\beta$ at any fixed non-zero wave vector $\mathbf{k}$, since $G(\mathbf{k})$ is a continuous function of $\mathbf{k}$ for $| \, \mathbf{k} \, | > 0$. Moreover, critical singularities are universal and, therefore, $\partial G(\mathbf{k})/\partial t$ exhibits such logarithmic singularity both in the lattice model and in the continuous model. The numerical analysis alone cannot provide a real proof that the discussed here singularities are exactly logarithmic. On the other hand, the singularity of $\partial G(\mathbf{k})/\partial t$ and the related asymptotic singularities could not be only approximately logarithmic, since $\partial G(\mathbf{k})/\partial t$ contributes to specific heat (28) (or (6), where $G(\mathbf{k}) - G^*(\mathbf{k}) = t \, \partial G(\mathbf{k})/\partial t$ holds at $t \to 0$ and $\mathbf{k} \neq \mathbf{0}$), but the singularity of specific heat is known to be exactly logarithmic for the models of 2D Ising universality class, including the scalar 2D φ^4 model.

According to the scaling hypothesis (7), the asymptotic small-t behavior of $\partial G(\mathbf{k})/\partial t$ can be reached only at $\xi \sim 1/k$, i. e., at $t \sim k$ in our case. Therefore, the asymptotic small-t behavior of $\Delta\Phi(\Lambda')$ in the thermodynamic limit is reached with a given accuracy at $t < t^*$, where $t^* \to 0$ at $\Lambda' \to 0$. It is consistent with the fact that the linearity of the $\Delta\Phi(\Lambda')$ vs $\ln t$ plot is better for $\Lambda' = 7\pi/8$ and $\Lambda' = 3\pi/4$ than for $\Lambda' = 5\pi/8$ in Fig. 3.

The logarithmic singularity of $\partial G(\mathbf{k})/\partial t$ implies that $\Delta\Phi(\Lambda') = \Phi(\pi) - \Phi(\Lambda')$ behaves as $\sim \ln t$ in the thermodynamic limit at $t \to 0$, as a result of an integration of $k \, \partial G(\mathbf{k})/\partial t$ over $\Lambda' < | \, \mathbf{k} \, | < \Lambda$ (according to (32) at $L \to \infty$). The same is true for $\Delta C_V^{sing}(\Lambda') = C_V^{sing} - C_V^{sing}(\Lambda')$ with the singular part of specific heat C_V^{sing} given by (28), $C_V^{sing}(\Lambda')$ being the contribution of the integration region $k < \Lambda'$. Hence we find $C_V^{sing}(\Lambda') \sim \ln t$, using the fact that $C_V^{sing} \sim \ln t$ holds in the actual 2D φ^4 model. Since $C_V^{sing}(\Lambda')$ in the theorem is defined as the leading singular contribution of the $k < \Lambda'$ region at $t \to 0$, represented in powers of ξ and $\ln \xi$, we have $C_V^{sing}(\Lambda') \propto \ln \xi$. Consequently, the condition of the theorem $C_V^{sing}(\Lambda') = A(\Lambda') \, (\ln \xi)^\lambda \xi^{\alpha/\nu}$ is satisfied here with $\lambda = 1$ and $\alpha = 0$.

As discussed before, the long–wavelength (small-k) contributions, i. e., $\Phi(\Lambda')$ and $C_V^{sing}(\Lambda')$ at small Λ' values, have similar singularities. The logarithmic singularity of $C_V^{sing}(\Lambda')$ thus means that $\Phi(\Lambda') = \mathcal{B}_1(\Lambda') \ln t$ holds with some coefficient $\mathcal{B}_1(\Lambda')$ for small cut-off parameter Λ' in the thermodynamic limit at $t \to 0$. Moreover, since $\partial G(k)/\partial t$

16

has a logarithmic singularity at any fixed positive k in this limit, the asymptotic relation $\Phi(\Lambda') = \mathcal{B}_1(\Lambda') \ln t$ can be extended (by integrating $k \partial G(k)/\partial\beta$ over k) to any finite value of Λ' not exceeding Λ. We have also a similar asymptotic relation $\Delta\Phi(\Lambda') = \mathcal{B}_2(\Lambda') \ln t$ for $\Delta\Phi(\Lambda')$, as consistent with our earlier statements. It yields $\Phi = \mathcal{B} \ln t$ with $\mathcal{B} = \mathcal{B}_1(\Lambda') + \mathcal{B}_2(\Lambda')$ for $\Phi = \Phi(\Lambda') + \Delta\Phi(\Lambda')$ in the thermodynamic limit at $t \to 0$. As an extra argument, the plots in Figs. 2 and 3 provide a direct numerical evidence that these relations and logarithmic singularities really hold true. It is clear from Fig. 2 that $\mathcal{B} < 0$ holds, since the asymptotic slope of the plot (for $tL \to \infty$) is negative. On the other hand, $\partial G(k)/\partial\beta$ is negative at $t \to 0$ for any fixed Λ' in the thermodynamic limit, according to the scaling behavior shown in Fig. 4, where $\partial G(k)/\partial\beta < 0$ holds for $k > k^*(t)$ with $k^*(t)$ tending to zero approximately as $\propto t$ at $t \to 0$. It means that $\mathcal{B}_2(\Lambda') > 0$ holds. In such a way, we have $\mathcal{B}_1(\Lambda') = \mathcal{B} - \mathcal{B}_2(\Lambda') < \mathcal{B}$ and thus $\lim_{\Lambda' \to 0} \mathcal{B}_1(\Lambda') \neq 0$, i. e., the long–wavelength contribution to Φ is relevant. Consequently, the corresponding (similar) long–wavelength contribution to C_V^{sing} is also relevant, implying that the condition of the theorem $\lim_{\Lambda' \to 0} A(\Lambda') \neq 0$ is satisfied.

6   Monte Carlo analysis

6.1   Relations of finite–size scaling

According to the finite–size scaling theory, susceptibility can be represented as

$$\chi = L^{\gamma/\nu} \left(f_0(L/\xi) + f_1(L/\xi) L^{-\omega} + \cdots \right) + \chi_{\mathrm{anal}}(t, L) , \tag{34}$$

where $f_i(L/\xi)$ are scaling functions, ω is the leading correction–to–scaling exponent, and $\chi_{\mathrm{anal}}(t, L)$ is the analytical background contribution. The singular part of $\partial U/\partial\beta$ can be represented in a similar way as that of χ with the scaling exponent $1/\nu$ instead of γ/ν. The scaling argument L/ξ tends to a constant at $\beta = \widetilde{\beta}_c(L)$ and $L \to \infty$. Consequently, if the actual φ^4 model is described by the same critical exponents $\gamma = 7/4$ and $\nu = 1$ as the 2D Ising model, then $\chi/L^{7/4}$ and $(\partial U/\partial\beta)/L$ at $\beta = \widetilde{\beta}_c(L)$ tend to some nonzero constants at $L \to \infty$. The data in Tabs. 1 to 6 are consistent with this idea. The L–dependence of $\chi/L^{7/4}$ and $(\partial U/\partial\beta)/L$ is caused by corrections to scaling, including those coming from the analytic background term, if it exists. Thus, we have

$$\chi/L^{7/4} = a_0 + \sum_{k \geq 1} a_k L^{-\omega_k} , \tag{35}$$

$$\frac{1}{L}\frac{\partial U}{\partial\beta} = b_0 + \sum_{k \geq 1} b_k L^{-\omega_k} \tag{36}$$

for large L at $\beta = \widetilde{\beta}_c(L)$, where a_k and b_k are expansion coefficients and ω_k are correction–to–scaling exponents. The existence of trivial corrections to scaling with integer ω_k is expected, since such corrections appear in the 2D Ising model.

The numerical analysis in [15] indicates that the susceptibility of the 2D Ising model on various lattices contains logarithmic corrections, coming from the "short–distance" contribution of the form

$$B^{\mathrm{lattice}} = \sum_{q=0}^{\infty} \sum_{p=0}^{[\sqrt{q}]} b^{(p,q)} (\ln |t|)^p t^q . \tag{37}$$

These terms with $p > 0$ in (37) represent a correction of order $O(t \ln | t |)$, which is a quantity of order $O(\ln L/L)$ in the finite–size scaling regime $t \sim 1/L$. These are high–order correction terms, which are not included in our fits, since the leading of them is by a factor $\sim L^{-11/4} \ln L$ smaller than the susceptibility χ at $L \to \infty$.

The singular terms in (34), which are not related to (37), will be further referred as the "long–distance" singular contributions. According to [15], these are representable by integer correction exponents in (34) at $L/\xi \to \infty$ in the case of the 2D Ising model. This is usually expected to be true also at finite values of L/ξ. Thus, if corrections to scaling in the scalar 2D φ^4 model have such structure, then (35) contains corrections $a_1 L^{-1}$, $a_2 L^{-7/4}$, $a_3 L^{-2}$ and corrections of higher orders. Moreover, in this case we have $a_2 = \chi_{\text{anal}}(0, \infty)$, so that the coefficient a_2 is independent of the particular choice of $\widetilde{\beta}_c(L)$, i. e., choice of U. Following the analogy with 2D Ising model, one can expect that a_1 vanishes at $\beta = \beta_c$ and, therefore, probably also at $U = U^*$. In distinction from susceptibility, $\partial U/\partial \beta$ does not contain such a constant contribution, which comes from an analytical background term, since U is constant ($U = 3$ at $\beta < \beta_c$ and $U = 1$ at $\beta > \beta_c$) at $\beta \neq \beta_c$ and $L \to \infty$. A constant contribution can, nevertheless, exist as a correction to the leading singular term.

6.2   Preliminary finite–size scaling analysis of the data

Summarizing the discussion in Sec. 6.1, we conclude that the $\chi/L^{7/4}$ vs $1/L$ plots are asymptotically linear at $L \to \infty$ for $U \neq U^*$ in the case of the Ising scenario, i. e., if the structure of corrections to scaling in the scalar 2D φ^4 model is similar to that one expected in the 2D Ising model. The asymptotic linearity of the $\chi/L^{7/4}$ vs $L^{-7/4}$ plots can be expected in the special case of $U = U^*$. Our MC results support the idea that this really corresponds to the Ising scenario, since the $\chi/L^{7/4}$ vs $L^{-7/4}$ rather than $\chi/L^{7/4}$ vs L^{-1} plot is almost linear for $U = 1.1679229 \approx U^*$ at $\lambda = 10$, i. e., close to the Ising limit. The discussed here plots are shown in Fig. 5, using the $1/L$ scale for $U = 2$ and $L^{-7/4}$ scale for $U \approx U^*$. The plots at $\lambda = 0.1$ and $\lambda = 1$ are remarkably nonlinear, whereas those at $\lambda = 10$ look more linear. The latter, however, is not surprising, since the Ising limit is approached at large values of λ. The best linearity is observed at $\lambda = 10$ and $U = 2$, where the χ^2/d.o.f. of the linear fit within $8 \leq L \leq 256$ is 2.33.

The asymptotic (large-L) linearity of the $-(\partial U/\partial \beta)/L$ vs $1/L$ plots can be expected according to the Ising scenario. However, if the coefficient at $1/L$ vanishes for $U = U^*$ (as it is, probably, true for $\chi/L^{7/4}$ in the 2D Ising model), then the asymptotic linearity of $-(\partial U/\partial \beta)/L$ vs L^{-2} plots is expected in this particular case. The $-(\partial U/\partial \beta)/L$ vs $1/L$ plots for $U = 2$ are shown in Fig. 6, whereas $-(\partial U/\partial \beta)/L$ plots depending on $1/L$ and $1/L^2$ for $U = 1.1679229 \approx U^*$ are shown in Fig. 7. The best linearity is, again, observed at $\lambda = 10$ and $U = 2$. However, even in this case the quality of the $-(\partial U/\partial \beta)/L$ vs $1/L$ fit is low: χ^2/d.o.f. = 4.24.

The nonlinearity of the plots at $\lambda = 0.1$ and $\lambda = 1$ in Figs. 5 – 7 indicate that nontrivial corrections to scaling with different exponents than those expected in the 2D Ising model could exist. In this case, the approximate linearity of some of the plots at $\lambda = 10$ can be easily explained by the fact that the amplitudes of nontrivial correction terms vanish in the Ising limit $\lambda \to \infty$. The analysis of this section is preliminary, since it is based only on the evaluation of linearity of some plots. Nevertheless, we can expect from this analysis that the data for small values of λ (such as $\lambda = 0.1$), where the nonlinearity of these plots is more pronounced, give the best chance to identify nontrivial correction terms, if they really exist. Due to this reason, we have extended simulations up to $L = 1536$ at $\lambda = 0.1$
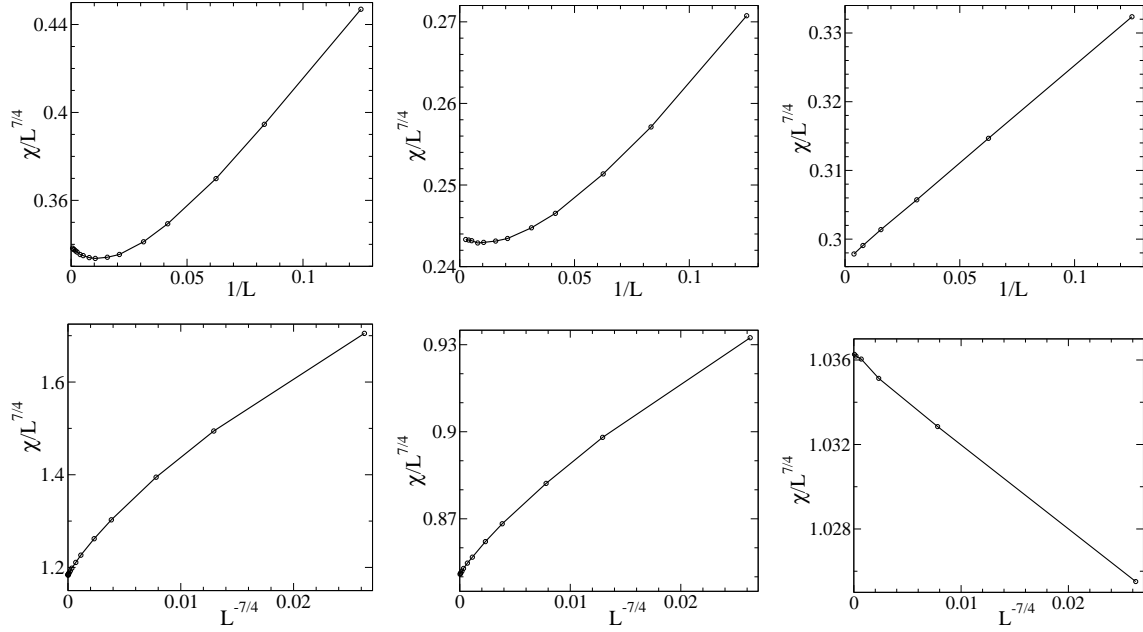
18

Figure 5: The $\chi/L^{7/4}$ vs $1/L$ plots for $U = 2$ (top) and $\chi/L^{7/4}$ vs $L^{-7/4}$ plots for $U = 1.1679229 \approx U^*$ (bottom) at $\lambda = 0.1$ (left), $\lambda = 1$ (middle) and $\lambda = 10$ (right). The range of sizes $L \geq 8$ is shown. Statistical errors are smaller than the symbol size.
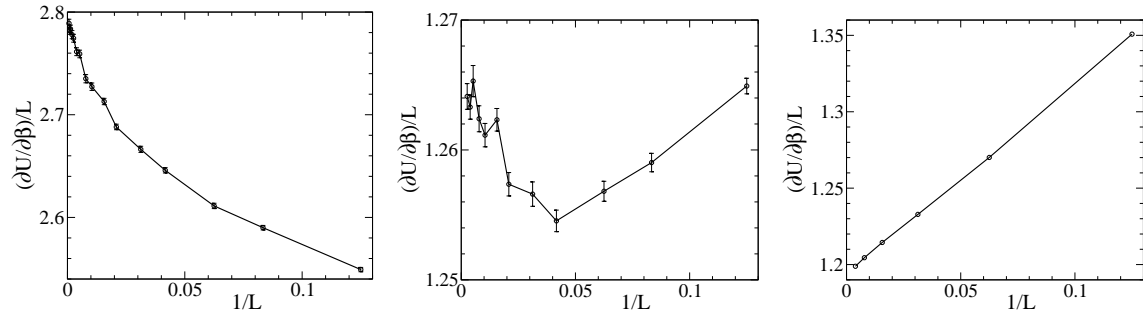

Figure 6: The $-(\partial U/\partial \beta)/L$ vs $1/L$ plots for $U = 2$ at $\lambda = 0.1$ (left), $\lambda = 1$ (middle) and $\lambda = 10$ (right). The range of sizes $L \geq 8$ is shown. Statistical errors at $\lambda = 10$ are smaller than the symbol size.
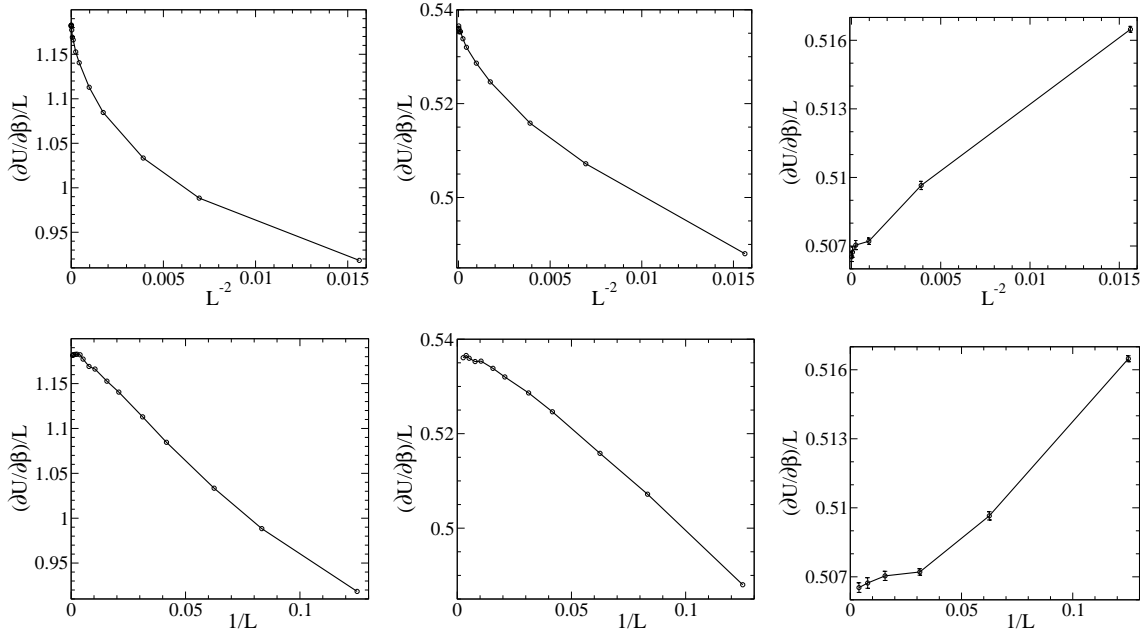
Figure 7: The $-(\partial U/\partial \beta)/L$ plots for $U = 1.1679229 \approx U^*$ depending on $1/L^2$ (top) and $1/L$ (bottom) at $\lambda = 0.1$ (left), $\lambda = 1$ (middle) and $\lambda = 10$ (right). The range of sizes $L \geq 8$ is shown. Statistical errors at $\lambda = 0.1$ and $\lambda = 1$ are about the symbol size or smaller.

and have performed a refined analysis of the data in this case – see Sec. 6.3.

6.3   Estimation of correction exponents

In order to estimate correction–to–scaling exponents, first we are looking for quantities, which can be well fit over a wide range of sizes to the ansatz of the form $A + BL^{-\omega}$, including only a single correction exponent ω. Obviously, the most serious estimation is possible at $\lambda = 0.1$, where the data up to $L = 1536$ are available. We have find that $(\partial U/\partial \beta)/L$ data at $\lambda = 0.1$ and $U = 2$ can be fairly well fit to this ansatz within $L \in [L_{\min}, 1536]$ for $L_{\min} \geq 16$. These fits give $\omega = 0.470(27)$ with $\chi^2/\text{d.o.f.} = 1.23$ at $L_{\min} = 16$, $\omega = 0.497(38)$ with $\chi^2/\text{d.o.f.} = 1.25$ at $L_{\min} = 24$ and $\omega = 0.546(52)$ with $\chi^2/\text{d.o.f.} = 1.19$ at $L_{\min} = 32$. These values of ω are close to $1/2$. Intuitively, the exact value is expected to be a simple rational number, since all known critical exponents of the 2D Ising universality class are such numbers. Thus, the leading correction–to–scaling exponent in the scalar 2D φ^4 model can be just $\omega = 1/2$. The actual $-(\partial U/\partial \beta)/L$ plot depending on $L^{-1/2}$ is shown in Fig. 8. This plot is approximately linear within the whole range of sizes $4 \leq L \leq 1536$. The fit with fixed exponent $\omega = 1/2$ is fairly good within $16 \leq L \leq 1536$. This fit with $\chi^2/\text{d.o.f.} = 1.22$ is shown in Fig. 8 by straight line.

A reasonable explanation of these results is such that (36) contains a term with the exponent $1/2$, which is the leading term within $16 \leq L \leq 1536$, at least, for the actual parameters $\lambda = 0.1$ and $U = 2$. According to the analytical arguments in Sec. 2, a correction term with exponent $3/4$ exists in the two–point correlation function. Thus, it is expected in (35) – (36), as well. As explained in Sec. 2, extra correction terms with
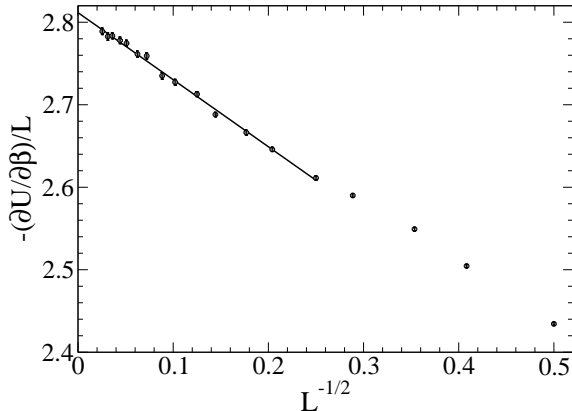
Figure 8: The $(\partial U/\partial \beta)/L$ vs $L^{-1/2}$ plot for $\lambda = 0.1$ and $U = 2$. The straight line represents the fit to $A + BL^{-1/2}$ within $16 \leq L \leq 1536$.

smaller exponents are also possible. The current analysis provides an evidence for such a correction with exponent $1/2$. According to the predictions of [6], a correction term with exponent $1/4$ is also expected. Our analysis of these data does not provide any evidence for such a correction. However, there is no contradiction with this conception, if we assume that the amplitude of the latter correction term is relatively small. In this case the behavior in Fig. 8 should be changed for large enough lattice sizes to the $\sim L^{-1/4}$ asymptotic convergence.

This scenario is supported by the $(\partial U/\partial \beta)/L$ data at $\lambda = 0.1$ and $U = 1.1679229 \approx U^*$. These data are not well described by $A + BL^{-\omega}$, but can be quite well fit to a refined ansatz of the form $A + BL^{-\omega} + CL^{-2\omega}$. The exponent $\omega = 1/4$ would confirm the aforementioned scenario. The data for $\lambda = 0.1$ and $U = 1.1679229 \approx U^*$ are satisfactory well fit to this ansatz within $L \in [48, 1536]$, yielding $\omega = 0.275(79)$. The χ^2/d.o.f. of this fit is 1.08, which is the smallest value among all fits within $[L_{\min}, 1536]$, for which the number of degrees of freedom exceeds the number of fit parameters (i. e., for $L_{\min} \leq 96$). This result is well consistent with $\omega = 1/4$. Other estimates are $\omega = 0.399(22)$ for $L_{\min} = 16$, $\omega = 0.436(46)$ for $L_{\min} = 24$, $\omega = 0.386(59)$ for $L_{\min} = 32$ and $\omega = 0.26(11)$ for $L_{\min} = 64$ with χ^2/d.o.f. $= 1.24, 1.24, 1.23$ and 1.24, respectively. We have performed also fits within $L \in [L_{\max}/32, L_{\max}]$ with different maximal lattice sizes $L_{\max}$. The results are $\omega = 0.477(77)$ for $L_{\max} = 768$, $\omega = 0.394(78)$ for $L_{\max} = 1024$ and $\omega = 0.275(79)$ for $L_{\max} = 1536$ with χ^2/d.o.f. $= 1.48, 1.40$ and 1.08, respectively. These ω values tend to decrease when the lattice sizes are increased, showing that ω can be as small as $1/4$. Another possibility is that ω has a larger value, closer to $\omega = 0.399(22)$, provided by the wide–range fit over $L \in [16, 1536]$.

As an extra test, we have fit these $(\partial U/\partial \beta)/L$ data at $\lambda = 0.1$ and $U = 1.1679229 \approx U^*$ to the ansatz $A + BL^{-1/2} + CL^{-\omega}$, where one of the correction exponents is set equal to $1/2$, in agreement with the behavior in Fig. 8. The fit within $L \in [48, 1536]$ is fairly good (χ^2/d.o.f. $= 1.07$) and gives $\omega = 0.34(26)$. It is consistent with our previous estimations, although the error bars are larger.

The analysis of corrections to scaling contained in $\chi/L^{7/4}$ is a more difficult problem than the actual analysis of the $(\partial U/\partial \beta)/L$ data, since the susceptibility χ contains a constant background contribution. The necessity to consider several correction terms

Table 7: The fit parameters a_1 and a_2 in (38) depending on the fit interval $L \in [\bar{L}/8, 8\bar{L}]$ for the $\chi/L^{7/4}$ data with $U = 1.1679229 \approx U^*$ in Tab. 2. The values of a_2 for the data with $U = 2$ in Tab. 1 are denoted by a_2^*, and Δa_2 is the difference $a_2 - a_2^*$. The values of χ^2/d.o.f. of the fits are shown in columns No. 4 and 7 for $U = 1.1679229$ and $U = 2$, respectively.

$\bar{L}$	a_1	a_2	χ^2/d.o.f.	a_2^*	Δa_2	χ^2/d.o.f.
64	0.239(26)	59.16(69)	3.99	30.31(46)	28.84(82)	3.06
96	0.104(37)	64.6(1.3)	1.60	33.95(88)	30.6(1.6)	2.29
128	0.065(45)	66.5(2.0)	1.43	37.9(1.4)	28.6(2.4)	0.96
192	0.039(65)	68.8(3.8)	1.45	40.8(2.8)	28.0(4.7)	0.90

makes the estimation of correction exponents ambiguous. Due to this reason, we have only performed some consistency tests with fixed exponents for χ, as described in Sec. 6.4.

6.4 Test of the Ising scenario

We have fit our susceptibility data for $\lambda = 0.1$ within $L \in [\bar{L}/8, 8\bar{L}]$ at different values of $\bar{L}$, using the ansatz

$$\frac{\chi}{L^{7/4}} = a_0 + a_1 L^{-1} + a_2 L^{-7/4} + a_3 L^{-2} \tag{38}$$

in order to test the consistency of the coefficients a_1 and a_2 with the Ising scenario discussed in Secs. 6.1 and 6.2. Namely, if corrections to scaling have the same structure as expected in the 2D Ising model, then (38) holds at $L \to \infty$ with U–independent value of a_2. The results depending on $\bar{L}$ are collected in Tab. 7. As we can see, a_1 for $U \approx U^*$ tends to zero with increasing of the lattice sizes used in the fit, i. e., with increasing of $\bar{L}$. It can be, indeed, expected in the Ising scenario. The coefficient a_2 is slightly varied with $\bar{L}$ for both $U = 1.1679229 \approx U^*$ and $U = 2$. The difference Δa_2 between the values of a_2 in these two cases, however, is rather stable and clearly inconsistent with zero. Thus, the Ising scenario, where $\Delta a_2 \to 0$ at $\bar{L} \to \infty$, is not confirmed.

We have performed also the tests at $\lambda = 1$. In this case, the data are fairly well fit within $L \in [8, 384]$, yielding $a_1 = 0.036(10)$ and $a_2 = 8.10(26)$ with χ^2/d.o.f. $= 1.26$ for $U = 1.1679229 \approx U^*$, and $a_2 = 5.11(18)$ with χ^2/d.o.f. $= 1.17$ for $U = 2$. The fits within $L \in [12, 384]$ yield $a_1 = 0.028(18)$ and $a_2 = 8.37(59)$ with χ^2/d.o.f. $= 1.40$ for $U = 1.1679229$, and $a_2 = 5.75(40)$ with χ^2/d.o.f. $= 0.87$ for $U = 2$. As we can see, the coefficient a_1 is marginally well consistent with zero, whereas the values of the coefficient a_2 for $U \approx U^*$ and $U = 2$ are inconsistent, as in the case of $\lambda = 0.1$.

If the singular "long–distance" terms in susceptibility (34) (see the discussion in Sec. 6.1) contain only integer correction–to–scaling exponents, then a_2 comes from the analytical background contribution and, thus, must be U–independent. Consequently, the failure in our consistency tests strongly suggests that theses singular terms contain non-trivial corrections to scaling, described by non–integer correction–to–scaling exponents. If the expansion of $\chi/L^{7/4}$ contains all positive integer powers of $L^{-1/4}$, then both singular and analytical parts of susceptibility χ contribute to the coefficient at $L^{-7/4}$ and, therefore, this coefficient is U–dependent.

Table 8: The fitted values of the exponent ω in (39) depending on $L_{\min}$ for fits within $L \in [L_{\min}, 1536]$. The quality of the fits is characterized by quantities $\chi^2/$d.o.f. (χ^2 per degree of freedom) and Q (goodness of the fit).

$L_{\min}$	ω	$\chi^2/$d.o.f.	Q
6	1.188(15)	4.11	0.00000074
8	1.299(25)	1.67	0.066
12	1.373(48)	1.50	0.123
16	1.418(81)	1.60	0.099
24	1.40(14)	1.78	0.066

We have performed one more test of the Ising scenario, using the $\partial U/\partial \beta$ data at $U = 1.1679229 \approx U^*$. According to this scenario, a non-vanishing term $\propto L^{-2}$ is always expected in (36). Therefore we have fit these data to

$$\frac{1}{L}\frac{\partial U}{\partial \beta} = A + BL^{-2} + CL^{-\omega} \tag{39}$$

to test how well the extra exponent ω is consistent with an integer value, which is different from 2, as it must be true if the Ising scenario holds. The results for ω depending on the fit interval $L \in [L_{\min}, 1536]$ are collected in Tab. 8. The values of $\chi^2/$d.o.f., as well as the values of the goodness Q of the fit [26] in Tab. 8, show that these fits have a rather low quality. In fact, only the fits with $Q > 0.1$ are normally accepted [26], so that only the fit with $L_{\min} = 12$ is more or less acceptable, and $\omega = 1.373(48)$ is the best estimate in Tab 8. We have skipped the results for $L_{\min} > 24$, since these fits are not better and have remarkably larger statistical errors. The low quality of the fits indicate that (39), probably, is not the correct asymptotic ansatz. Moreover, the estimated values of ω and the best estimate $\omega = 1.373(48)$ are inconsistent with any integer value. Thus, the Ising scenario is, again, not confirmed.

7   Summary and conclusions

Corrections to scaling in the scalar 2D φ^4 model have been studied based on non-perturbative analytical arguments and Monte Carlo analysis. The analytical results are based on certain scaling assumptions and the theorem proven in Sec. 2. Important conditions of the theorem have been numerically tested and confirmed in Sec. 5, using the Monte Carlo results described in Secs. 3 and 4.

Our analysis supports the finite–size corrections near criticality, representable by an expansion of a correction factor in powers of $L^{-1/4}$. Following [15], we allow that some of high–order expansion terms in the scalar 2D lattice φ^4 model can be modified to include logarithmic factors. Analytical arguments show the existence of corrections with the correction–to–scaling exponent $3/4$. A brief review of finite–size scaling relations and preliminary MC analysis of the data are provided in Secs. 6.1 – 6.2. The MC analysis of the $(\partial U/\partial \beta)/L$ data in Sec. 6.3 provides an evidence that there exist corrections with the exponent $1/2$ and, very likely, also corrections with the exponent about $1/4$. The

numerical tests in Sec. 6.4 clearly show that the structure of corrections to scaling in the 2D φ^4 model differs from that one expected in the 2D Ising model.

The overall behavior of the $(\partial U/\partial \beta)/L$ and $\chi/L^{7/4}$ data can be interpreted in such a way that nontrivial corrections in the form of the expansion in powers of $L^{-1/4}$ generally exist, although corrections with $\omega_k < 1$ in (35) and (36) can be well detectable only for small values of λ, such as $\lambda = 0.1$, since the amplitudes of these correction terms decrease with increasing of λ and approaching the Ising limit $\lambda \to \infty$. It naturally explains the fact that some of the plots at $\lambda = 10$, discussed in Sec. 6.2, are almost linear, as it is expected in the 2D Ising model.

Apart from corrections to scaling, we have estimated the critical coupling β_c depending on λ in Sec. 4 and have discussed an interesting phenomenon that the critical temperature $(1/\beta_c)$ appears to be a non-monotonous function of λ.

Acknowledgments

References

[1] D. J. Amit, *Field Theory, the Renormalization Group, and Critical Phenomena*, World Scientific, Singapore, 1984.

[2] S. K. Ma, *Modern Theory of Critical Phenomena*, W. A. Benjamin, Inc., New York, 1976.

[3] J. Zinn-Justin, *Quantum Field Theory and Critical Phenomena*, Clarendon Press, Oxford, 1996.

[4] H. Kleinert, V. Schulte-Frohlinde, *Critical Properties of ϕ^4 Theories*, World Scientific, Singapore, 2001.

[5] A. Pelissetto, E. Vicari, Phys. Rep. 368 (2002) 549–727.

[6] J. Kaupužs, Ann. Phys. (Berlin) 10 (2001) 299–331.

[7] J. Kaupužs, Int. J. Mod. Phys. A 27, 1250114 (2012)

[8] J. Kaupužs, Canadian J. Phys. **9**, 373 (2012)

[9] A. Milchev, D. W. Heermann, K. Binder, J. Stat. Phys. **44**, 749 (1986)

[10] R. Toral, A. Chakrabarti, Phys. Rev. B **42**, 2445 (1990)

[11] B. Mehling, B. M. Forrest, Z. Phys. B **89**, 89 (1992)

[12] R. Kenna, D. A. Johnston, W. Janke, Phys. Rev. Lett. **97**, 155702 (2006); Erratum – ibid **97**, 169901 (2006)

[13] J. Kaupužs, Int. J. Mod. Phys. C **17**, 1095 (2006)

[14] H. Au-Yang, J. H. H. Perk, Int. J. Mod. Phys. B **16**, 2089 (2002)

[15] Y. Chan, A. J. Guttman, B. G. Nickel, J. H. H. Perk, J. Stat. Phys. **145**, 549 (2011)

[16] M. Caselle, M. Hasenbusch, A. Pelissetto, E. Vicari, J. Phys. A **35**, 4861 (2002)

[17] J. Salas, A. D. Sokal, J. Stat. Phys. **98**, 551 (2000)

[18] W.P. Orrick, B. Nickel, A.J. Guttmann and J.H.H. Perk, J. Stat. Phys. **102**, 795 (2001)

[19] A. Aharony, M. E. Fisher, Phys. Rev. Lett. **45**, 679 (1980)

[20] A. Aharony, M. E. Fisher, Phys. Rev. B **27**, 4394 (1983)

[21] M. Barma, M. Fisher, Phys. Rev. Lett. **53**, 1935 (1984)

[22] M. Hasenbusch, J. Phys. A: Math. Gen. **32**, 4851 (1999)

[23] M. E. J. Newman, G. T. Barkema, Monte Carlo Methods in Statistical Physics, Clarendon Press, Oxford, 1999

[24] J. Kaupužs, J. Rimšāns, R. V. N. Melnik, Phys. Rev. E **81**, 026701 (2010).

[25] J. Kaupužs, J. Rimšāns, R. V. N. Melnik, Ukr. J. Phys. 56, 845 (2011)

[26] W. H. Press, B. P. Flannery, S. A. Teukolsky, W. T. Vetterling, Numerical Recipes – The Art of Scientific Computing, Cambridge University Press, Cambridge, 1989

[27] R. J. Baxter, *Exactly Solved Models in Statistical Mechanics*, Academic Press, London, 1989.

[28] M. Hasenbusch, Int. J. Mod. Phys. C **12**, 911 (2001).